



Research Article

## Experimental study on energy-saving effect of alternate temperature system with cold storage unit

Leilei Zhu <sup>a</sup>, Jiren Li <sup>b</sup>, Houlei Zhang <sup>\*,c</sup>

School of Energy and Power Engineering, Nanjing University of Science and Technology, Nanjing, P R China

### Article Info

### Abstract

#### Article History:

Received 11 Apr 2025

Accepted 13 June 2025

#### Keywords:

Alternate temperature;  
Cold storage;  
Energy-saving

Alternate temperature systems with variable cooling load are commonly found in many applications, such as environmental tests. In this paper, we incorporate an ice-cold storage unit (i.e., a new design degree of freedom) into an alternate temperature system, and present an experimental study on the energy-saving effect of the design with cold storage. The cold storage energy comes from a part of the refrigerant bypass loss. Two lab-scale prototypes were developed and the work consumption of the system with cold storage was compared to that without cold storage. The experiment shows that the incorporation of the cold storage unit significantly reduces the energy consumption. Under the specified nominal design conditions, the compressor consumes 5.32 kWh/period energy for the design without cold storage, while it consumes only 3.77 kWh/period energy for the design with cold storage due to less compressor operating time. Compared with the design without cold storage, the energy consumption reduction ratio ( $\alpha$ ) of the design with cold storage reaches approximately 24.7%. When the heat capacity of the load increases, e.g., from 6.84 kJ/°C to 20.66 kJ/°C, the energy-saving effect of the design with cold storage becomes weaker, e.g.,  $\alpha$  decreasing from 24.7% to 20.8% accordingly. For extremely low heat generation in the load, the energy-saving effect of the design with cold storage diminishes. The effects of the fan's operating frequency and the cold-water temperature are also analyzed. Further design improvement is suggested. This work emphasizes the value of the incorporation of cold storage (i.e., adding more design degrees of freedom) for alternate temperature systems which reduces the heat transfer difference and the entropy generation.

© 2025 MIM Research Group. All rights reserved.

## 1. Introduction

Alternate temperature systems with strict temperature variation processes are widely used in reliability tests of electronic instruments with internal heat generation [1-4]. Figure 1 shows a typical alternate temperature process that comprises four stages, which is commonly applied in environmental test chambers [5]. Usually, the high temperature  $T_H$  is higher than the ambient temperature  $T_0$ , and the low temperature  $T_L$  is below  $T_0$ . In this paper,  $T_L$  is assumed less than  $T_{CS0}$  (0°C, the melting point of ice). In this case both heating and cooling are necessary. Since the duration of the rising temperature stage (i.e., Stage II) and the falling temperature stage (i.e., Stage IV) is much shorter than that of the two constant temperature stages (i.e., Stage I and Stage III), the cooling rate is highly imbalanced within one cycle. This imbalance in cooling rate demand requires the maximum capacity in Stage IV, which determines the size of the refrigeration device (or the compressor). In Stages other than Stage IV, the refrigeration device operates under part-load

\*Corresponding author: [houlei zhang@aliyun.com](mailto:houleizhang@aliyun.com)

<sup>a</sup>orcid.org/0009-0001-3972-1134; <sup>b</sup>orcid.org/0009-0006-9858-3102; <sup>c</sup>orcid.org/0000-0002-8980-5416

DOI: <http://dx.doi.org/10.17515/resm2025-814st0411rs>

Res. Eng. Struct. Mat. Vol. x Iss. x (xxxx) xx-xx

conditions with low energy efficiency.

The most widely used cooling method is based on vapor compression refrigeration, either single-stage or multi-stage systems [6,7]. To meet the cooling rate demand accurately, constant-speed vapor compression (CSVC) with refrigerant bypass adjustment offers a cost-effective solution in terms of equipment investment but comes with significant bypass energy losses. Both single- and multi-compressor designs incorporating refrigerant bypass adjustment are used in practice [8]. A more expensive variable-speed vapor compressor can improve energy efficiency under part-load conditions, but it does not fully eliminate the part-load issue [9, 10]. Beyond these methods, cold storage technology provides an alternative solution to address the imbalance between cooling supply and demand.

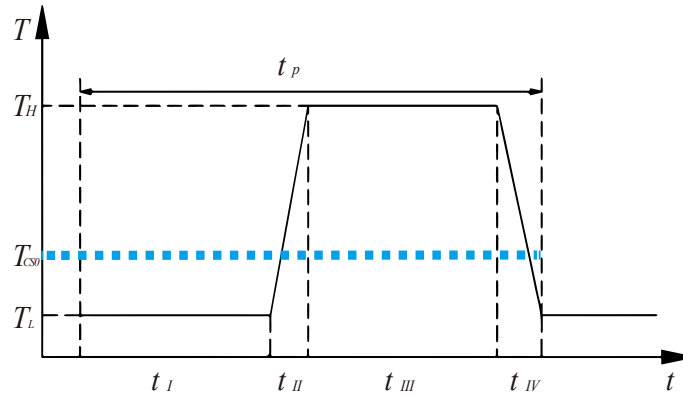


Fig. 1. Alternate temperature process [5]

In building air conditioning systems, cold storage has been employed for many years to reduce peak-hour utility consumption [11-14], and single-phase materials or phase change materials (PCMs) are commonly used to minimize temperature fluctuations and enhance energy efficiency. Recently, Rahgozar et al. [15] analyzed the economic feasibility of ice storage systems for office buildings. They highlight that the payback period is highly sensitive to climate conditions, storage strategies, and other factors. Conti et al. [16] presented a design method for heat storage-based heat pump system in building services to reduce partial-load losses. The electricity consumption may be reduced by up to 45% in a typical test case. Zhu et al. [17] proposed a model predictive control (MPC) strategy of a hybrid cooling system with a cold-water storage system in a data center, which can be regarded as a generalized form of a building with substantial internal heat generation. Their study optimized the cold storage tank volume, achieving a significant reduction in total annual energy consumption across multiple operational modes. Zhao et al. [18] developed a method coupled with multi-objective optimization and MPC for ice-storage air conditioning systems in building applications, showing that their optimization approach led to greater energy savings compared to storage-priority control. Lin et al. [19] employed a model-based control strategy utilizing deep learning to enhance chiller energy efficiency by leveraging the inherent cold storage capacity of cooling systems. Their test results indicated that this control strategy can reduce energy consumption during the nighttime and at the end of working hours markedly. References [17-19] underscore the importance of operational control and optimization when integrating cold storage technology.

PCMs-based cold storage has been also incorporated into refrigerators (including domestic appliances and cold-chain containers, etc.) to improve energy efficiency and product quality. For instance, Azzouz et al. [20, 21] showed a shorter compressor ON-time ratio and therefore a higher *COP* for domestic refrigerators with PCM cold storage. Marques et al. [22] recorded 19% energy-saving potential for domestic refrigerators with cold storage. Khan et al. [23] tested the performance improvement of a household refrigerator with PCM. The *COP* is improved around 20-27%, depending on the types of PCM and thermal load. Marques et al. [24] investigated the design and operation of a thermal storage refrigerator. The effects of the compressor capacity and the PCM in the refrigerator were evaluated. The results showed that the integration of a well-designed PCM slab can reduce the compressor operating time. Liu et al. [25] reported a significant reduction in

both energy consumption and compressor ON-time ratio for an air-cooled domestic refrigerator with PCMs in both cooling and freezing chambers. Ezan et al. [26] studied the effect of a PCM slab inside a vertical beverage cooler numerically and showed that the PCM integration reduces the compressor ON-time. Cheng et al. [27] discussed three thermal storage designs in domestic refrigerators, i.e., heat storage condenser, cold storage evaporator and dual energy storage, and showed that dual energy storage achieves the highest energy savings. Joybari et al. [28] reviewed the research on domestic refrigerators with cold storage. In Ref. [29], Liao et al. used a mixed salt solution as the cold storage PCM and studied the cold storage performance of the phase change cold storage module for refrigerated containers. They defined two new performance indicators, i.e., the cold storage coefficient and the cold storage efficiency. The effects of the structure layout and the unit power on the phase change cold storage were discussed and proper (or optimal) parameters were recommended. Gao et al. [30] studied the application of a direct current refrigerator with a phase-change cold storage and mini-electrical storage. The results demonstrated the most energy-efficient and cost-effective On-Off mode. Besides the research and development in building air conditioning systems and refrigerators, very recently, Zhang et al. [31] reviewed the studies and applications of PCMs for cold storage in China. Ouaouja et al. [32] conducted a comprehensive review of PCMs for cold storage applications for multiple perspectives, such as energy efficiency, temperature stabilization, and product quality, etc. In particular, new biomass-based PCMs were evaluated in detail.

The above-mentioned studies involve various analytical/research tools. In addition, other analytical tools have also been employed to investigate cold storage and its applications. The Constructal law, a physical law proposed by Bejan in 1996 [33, 34], provided a new thinking method in helping improving performance of thermal systems, including multi-scale design (considering space, time or other parameters) and entropy generation minimization design of cold storage-based processes [35-38]. Radcenco et al. [35] analyzed the intermittent operation of a defrosting refrigerator and presented the optimal on/off frequency by using thermodynamic optimization method (entropy generation minimization). Zamfirescu and Bejan [36] applied constructal law to a tree-shaped network (a multi-scale design structure) for cold storage, and the design with the maximization of ice production per unit volume was obtained. Using entropy generation minimization as the optimization objective, Bi et al. [37] studied the charging and discharging processes in a gas-hydrate cold storage system. The optimal control strategy for the cold storage system was determined. Very recently, Tavakoli et al. [38] investigated the effects of internal sinusoidal fins and phase change materials on a thermal storage system by performing entropy generation analysis. The design that minimized entropy generation was identified.

In our previous work, inspired by constructal law and entropy generation minimization thoughts, we formulated a multi-source cooling design of alternate temperature systems [5], which incorporates multiple cold storage temperatures and one evaporating temperature to match the source temperature and demand temperature. Such design incorporates more degrees of freedom to improve the system's performance. Theoretically, it was shown that the design with cold storage can simultaneously reduce energy consumption and the size of the refrigeration device. In Ref. [39], an alternate temperature test chamber with ice cold storage (a special case of the multi-source cooling design in Ref. [5]) was studied through numerical modeling. In this context, each cold storage temperature adds one degree of freedom to the design compared to a system without cold storage. When cold water from the cold storage unit is used in Stage III (cf. Fig. 1), the compressor ON-time decreases and then the energy consumption is reduced. Both Refs. [5] and [39] are based on theoretical analysis with certain simplifying assumptions. In this paper, we present an experimental study on the energy-saving effect of a real alternate temperature system (i.e., an environmental test chamber with periodically varying temperature) with ice cold storage unit. The results are also compared with those of a system without cold storage.

## 2. Experimental Setup

### 2.1. Prototype development

Two prototypes were developed: Prototype A, representing the conventional design without cold storage and Prototype B, featuring the improved design with cold storage. The working principles of Prototypes A and B are shown in Fig. 2a and Fig. 2b respectively. The abbreviations in Fig. 2 are listed in Nomenclature. In Fig. 2a, a refrigerant bypass through the valve V is used to regulate the cooling capacity which leads to significant energy loss [5, 39]. In Stage I of Fig. 2b, the compressor operates to maintain the temperature of the chamber and store cold energy in the cold storage tank (CST) (V1, V2: open; V: open or closed) simultaneously. In Stage II of Fig. 2b, the compressor may either run or stop, depending on the load of the object (OBJ). In Stage III of Fig. 2b, CST supplies cooling capacity to the chamber through the coolant heat exchanger (CHE) (V3: open), allowing the compressor to remain off. In Stage IV of Fig. 2b, the compressor resumes operation to provide cooling capacity to drop the temperature in the chamber according to the temperature demand. A comparison between the two prototypes shows that Prototype B has a shorter compressor operating time than Prototype A (seen in Section 3.3), leading to reduced energy consumption. It is also feasible to discharge cold storage energy from CST to the chamber in the high temperature parts of Stages II and IV. But, usually  $t_{III}$  is typically much longer than  $t_{II}$  or  $t_{IV}$ , the energy-saving effect in Stage III is dominant. In this research, the cold storage energy was exclusively discharged and applied only in Stage III.

From Fig. 1, we know that the cooling rate demand (i.e., the cooling load) is different from that for normal air conditioning applications and refrigerators, e.g., the strict periodic temperature change (including fast temperature rising and falling stages) and the significant cooling load imbalance. For the systems in Fig. 2, the refrigerant bypass adjustment is used for cooling capacity control due to its cost-effective equipment investment. The cold storage energy in Fig. 2b comes from a part of the refrigerant bypass loss in Stage I. In this design, some previously “wasted” cold energy is recovered and therefore the compressor operating time is reduced, e.g., in Stage III. The experimental work based on the above key points is new, which was not explored in the studies reviewed before.

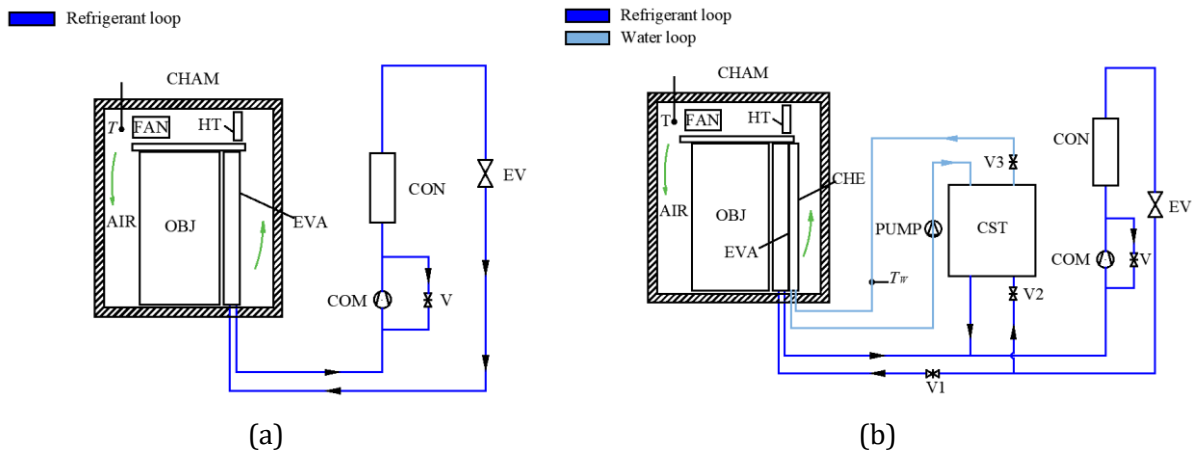


Fig. 2. Working principle: (a) prototype A; (b) prototype B

Two fin-and-tube ice-generating heat exchangers (IHEs) are installed in CST of Prototype B. The dimensions of an IHE are provided in Fig. 3a and its photo is shown in Fig. 3b. Photos of Prototypes A and B are presented in Fig. 4a and Fig. 4b respectively. The design parameters used for Prototypes A and B are summarized in Table 1.

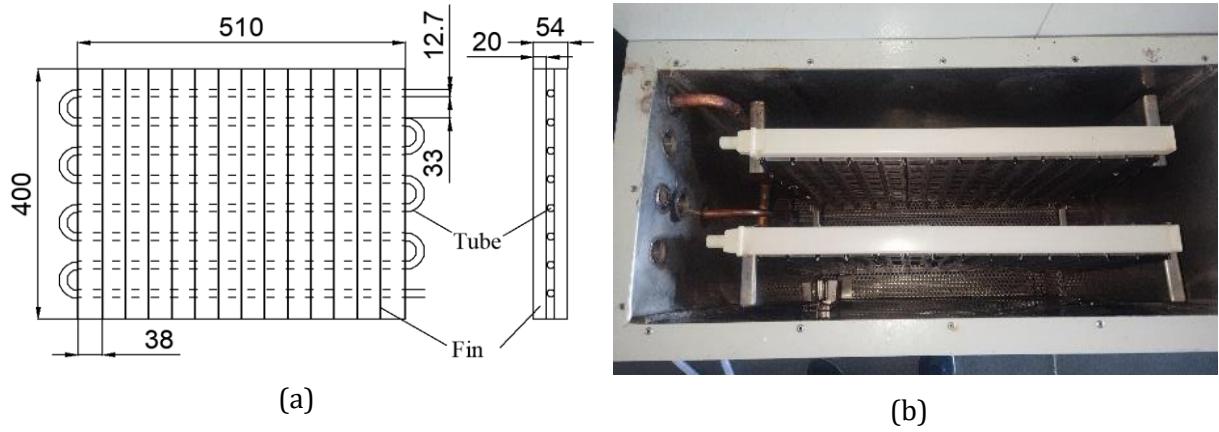


Fig. 3. Cold storage unit: (a) Dimensions (mm); (b) Photo of cold storage unit



Fig. 4. Photo of prototypes: (a) Prototype A; (b) Prototype B

Table 1. Design parameters of Prototypes A and B

Design parameters	Value
The size of OBJ in Prototypes A and B (Width×Height×Depth)	600 mm×850 mm×500 mm
The volume of the test space	225 L
The external dimension of Prototype (Width×Height×Depth)	800 mm×1970 mm×1360 mm (Prototypes A)
	800 mm×1970 mm×1960 mm (Prototypes B)
The total weight of Prototype	300 kg (Prototypes A)
	360 kg (Prototypes B)
Operating temperature range	-30°C~100°C
Temperature fluctuation	±1°C
Temperature deviation	±2°C
Temperature uniformity	≤2°C

## 2.2. Data Measurement and Analysis

To evaluate the energy-saving performance of Prototype B, the energy consumption reduction ratio and the compressor work reduction ratio are defined respectively as follows [5, 39].

$$\alpha = \frac{W_{t,A} - W_{t,B}}{W_{t,A}} \quad (1)$$

$$\beta = \frac{W_{c,A} - W_{c,B}}{W_{c,A}} \quad (2)$$

The total energy consumption  $W_t$  includes a few terms [40]:

$$W_t = W_c + W_h + W_f + W_p + W_e \quad (3)$$

where  $W_c$ ,  $W_h$ ,  $W_f$  and  $W_p$  represent the energy consumption of the compressor, the heater, the fan and the pump, respectively.  $W_e$  refers to all other energy consumption, except that consumed by the compressor, heater, fan and pump. For instance,  $W_e$  includes the energy consumption due to air leakage between the inside and the outside of the chamber, the heating energy that is used to remove frost on the surfaces of the inside walls of the chamber, and so on. This will be further discussed in the next section. By measuring  $W_b$ ,  $W_c$ ,  $W_h$ ,  $W_f$  and  $W_p$ ,  $W_e$  is calculated using Eq. (3). For Prototype A,  $W_p = 0$  since there is no water pump.

For both Prototypes A and B, the characteristic temperature (T) and the air velocity (v) in the chamber in front of OBJ are measured by a resistance temperature sensor (PT100) and an anemometer (Fluke 925 propeller flowmeter). For Prototype B, the water temperature is measured by K-type thermocouples. The water flow rate circulating between CST and CHE is measured by a vortex flowmeter. All data are acquired continuously and input into a computer for further analysis. The sensors used in the experiment are listed in Table 2.

Table 2. List of sensors

Sensor	Range	Accuracy
PT100	-50°C~+200°C	±0.5°C
K-type thermocouple	-40°C~+375°C	±1°C
Fluke 925 propeller flowmeter	0.4 m/s~25 m/s	±0.5 m/s
Electric power measurement YD2037Y-F	0 kW~6 kW	±0.02 kW
Vortex flowmeter KLWGY-DC-D6-W	0~0.6 m <sup>3</sup> /h	±0.05 m <sup>3</sup> /h

The uncertainty analysis is conducted following the methodology described by Moffat [41]. The absolute uncertainty associated with  $W_i$  ( $\delta(W_i)$ ) is 0.02kW at the 95% confidence level. The total energy consumption relative uncertainties ( $u(W_t)$ ) are calculated using Eq. (4), while the relative uncertainties of  $\alpha$  and  $\beta$  ( $u(\alpha)$ ,  $u(\beta)$ ) are derived from Eqs. (5) and (6) respectively. Under the specified nominal design conditions, i.e.,  $T_H = 70^\circ\text{C}$ ,  $T_L = -5^\circ\text{C}$ ,  $T_w = 2^\circ\text{C}$ ,  $f = 50$  Hz,  $Q = 1$  kW and  $C = 6.84$  kJ/°C, the relative uncertainties of  $W_{t,A}$ ,  $W_{t,B}$ ,  $\alpha$  and  $\beta$  are 0.75%, 1.11%, 4.08% and 0.95%, respectively. From the viewpoint of engineering applications, the uncertainties are acceptable.

$$u(W_t) = \frac{\sqrt{\left(\frac{\partial W_t}{\partial W_c} \delta W_c\right)^2 + \left(\frac{\partial W_t}{\partial W_h} \delta W_h\right)^2 + \left(\frac{\partial W_t}{\partial W_f} \delta W_f\right)^2 + \left(\frac{\partial W_t}{\partial W_p} \delta W_p\right)^2 + \left(\frac{\partial W_t}{\partial W_e} \delta W_e\right)^2}}{W_t} \quad (4)$$

$$u(\alpha) = \frac{1}{\alpha} \sqrt{\left(\frac{\partial \alpha}{\partial W_{t,A}} \delta W_{t,A}\right)^2 + \left(\frac{\partial \alpha}{\partial W_{t,B}} \delta W_{t,B}\right)^2} \quad (5)$$

$$u(\beta) = \frac{1}{\beta} \sqrt{\left(\frac{\partial \beta}{\partial W_{c,A}} \delta W_{c,A}\right)^2 + \left(\frac{\partial \beta}{\partial W_{c,B}} \delta W_{c,B}\right)^2} \quad (6)$$

### 3. Results and Discussion

#### 3.1. Nominal Design Conditions

First, we set the nominal design conditions as follows:  $T_H = 70^\circ\text{C}$ ,  $T_L = -5^\circ\text{C}$ ,  $T_w = 2^\circ\text{C}$ ,  $f = 50\text{ Hz}$ ,  $Q = 1\text{ kW}$  and  $C = 6.84\text{ kJ}/^\circ\text{C}$ . Among these parameters,  $T_H$  and  $T_L$  do not change in the experiment. Figures 5 and 6 show two examples of the temperature curves of Prototype A (the design without cold storage) and Prototype B (the design with cold storage) respectively for the nominal design conditions. The difference of the ambient conditions of the two tests is negligible. The two time-dependent temperature curves show negligible difference that means the two prototypes fulfill the same design requirement. It should be noted that at the end part of Stage IV, the temperature profile is not strictly linear, which does not affect the energy efficiency evaluation due to its very short time. This non-linearity can be reduced or eliminated in real products, although linear temperature dropping in Stage IV is not always necessary. Here the temperature control accuracy (i.e., the temperature fluctuation) is set as  $\pm 1^\circ\text{C}$ , and slight temperature fluctuations are observed.

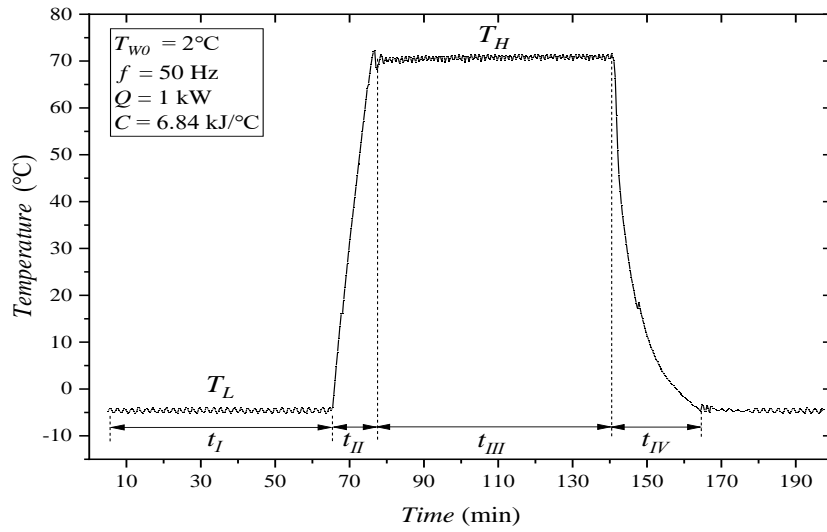


Fig. 5. Temperature curve of Prototype A under reference design conditions

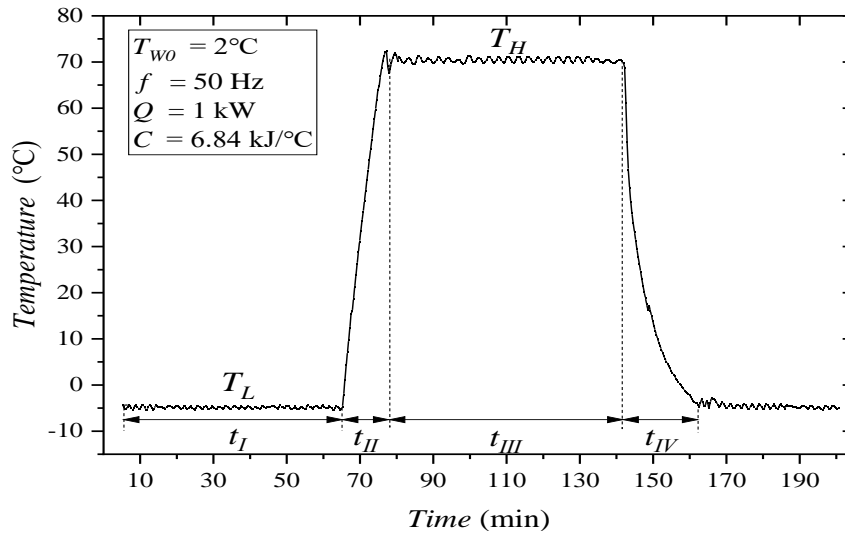


Fig. 6. Temperature curve of Prototype B under reference design conditions

For Prototype B, cold water from CST is used to cool the chamber in Stage III. The dynamic water temperature and flow rate are shown in Fig. 7, where  $T_w$  is the temperature at the inlet of CHE, and  $T_{w0}$  is the initial value of  $T_w$ . In Stage I and Stage II where the water pump does not run (i.e.,  $\dot{m}_w = 0$ ),  $T_w$  is lower ( $\sim 2^\circ\text{C}$ ) and changes very little. In Stage III where the water pump runs to provide cooling to the chamber through CHE,  $T_w$  becomes higher. The flow rate in Stage III varies

significantly because a large pump is used in building the prototype. In real product design, this can be optimized. The variation of  $T_w$  shows that the melting velocity of the ice in CST is slow which cannot maintain a constant water temperature. Heat transfer enhancement (e.g., using well-designed ice-side fins) in the ice melting process can help solve this problem, which will be studied in the future work.

Figure 8 shows the energy consumption distribution of the two prototypes under the nominal design conditions. In Stages III, as the compressor for Prototype B does not run, the energy saving is significant, and in this stage,  $W_t$  for Prototype B is much less than that for Prototype A. This is the main reason that the cold storage-based design saves energy overall the entire period. In Stage I, the energy consumption of the two prototypes is nearly the same. In Stage II, Prototype B consumes slightly less energy than Prototype A. In Stage IV, due to the cooling effect of cold water that is not fully discharged from CHE when the temperature starts to drop, Prototype B consumes less energy than Prototype A.

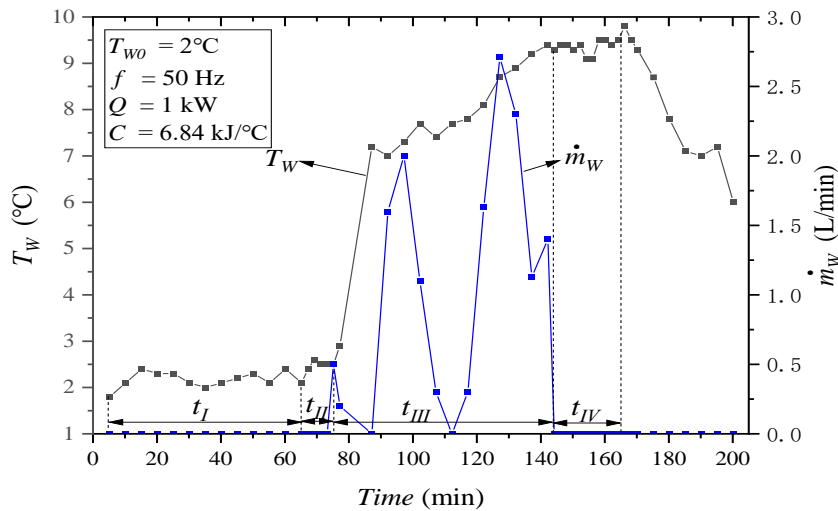


Fig. 7. Water temperature and flow rate of Prototype B under the nominal design conditions

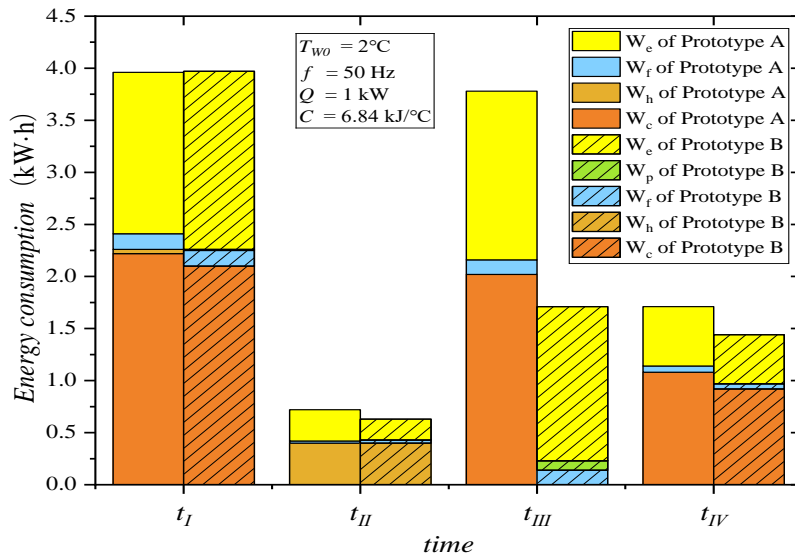


Fig. 8. Energy consumption distribution of Prototypes A and B under nominal design conditions

In one period, for Prototype A,  $W_c$ ,  $W_h$ ,  $W_f$  and  $W_e$  are 5.32 kWh, 0.44 kWh, 0.37 kWh and 4.04 kWh, respectively. Among the four terms,  $W_c$  (52.3% of the total) and  $W_e$  (39.7% of the total) are dominant, and  $W_h$  and  $W_f$  are much less. Here  $W_e$  includes the energy consumption due to air leakage, the heating energy for defrosting of the inner surfaces of the chamber and preventing condensation near the chamber door sealing zones, and the energy consumption for measurement

and control system. In the test procedure, humid air circulates in the chamber and frost emerges on the inner surfaces of the chamber when its temperature drops below 0°C. Electrical heaters attached to the surfaces run to remove the frost. Such frosting and defrosting processes occur periodically. It is possible to use dry air in the chamber as the circulating fluid which is not the focus of this work. Apparently, frosting and defrosting processes do not affect evaluating the goodness of the cold storage-based design. The importance of  $W_e$  is a reminder that the present prototypes (A and B) are not ideal, and there exists considerable improvement space.

In one period, for Prototype B,  $W_c$ ,  $W_h$ ,  $W_f$ ,  $W_p$  and  $W_e$  are 3.02 kWh, 0.40 kWh, 0.37 kWh, 0.10 kWh and 3.77 kWh, respectively.  $W_c$  and  $W_e$  are still dominant. By comparing the two prototypes, we see that  $W_h$  and  $W_e$  have a small gap. The energy consumption  $W_f$  is the same for the two prototypes which means that the incorporation of CHE does not increase the fan’s work. For Prototype B, the energy consumption of the water pump  $W_p$  is much less than  $W_c$ , so it is negligible in the energy consumption analysis. The key difference between Prototype A and Prototype B lies in  $W_c$ . Based on Fig. 8, the energy consumption reduction ratio ( $\alpha$ ) and the compressor work reduction ratio ( $\beta$ ) are 24.7% and 43.2%, respectively. The improvement in energy efficiency of Prototype B is significant. This result confirms our previous theoretical design [39].

### 3.2. Effects of Operating Conditions

Under the nominal design conditions in Section 3.1 (e.g., Fig. 8), the load heat capacity  $C = 6.84$  kJ/°C. Figures 9 and 10 show the energy consumption distribution for the load heat capacity  $C = 13.75$  kJ/°C and 20.66 kJ/°C respectively. Combined with Fig. 8, we see that in Stage IV (i.e., the temperature dropping process), with the increase of  $C$ , both  $W_c$  and  $W_i$  increase for both Prototype A and Prototype B. In fact, a larger heat capacity in the chamber is always detrimental to the temperature dropping process as more cold energy is needed. Stage III determines the energy-saving effect of Prototype B which does not change with  $C$  significantly. Considering the above two points (the features in Stage IV and III), we know that  $\alpha$  and  $\beta$  may decrease with the increase of  $C$  according to Eqs. (1) and (2). The test results of the effects of  $C$  are summarized in Fig. 11, which reveals that in the specified range cold storage-based design is more attractive for smaller load heat capacities.

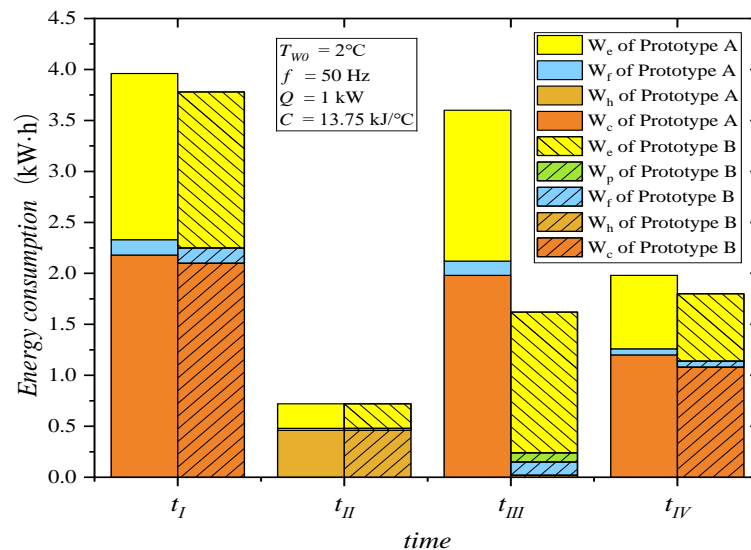


Fig. 9. Energy consumption distribution with  $C = 13.75$  kJ/°C

Another important parameter of the load is its internal heat generation  $Q$ . Usually the test is performed under the nominal design conditions (1 kW in this paper), but sometimes  $Q$  may be very small or even zero (non-working state of the load). Figure 12 shows the energy consumption distribution for the heat generation in the load  $Q = 0.2$  kW.

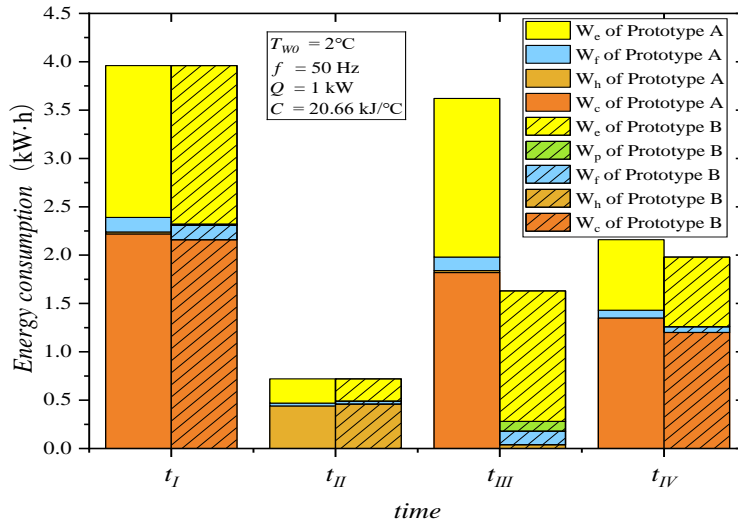


Fig. 10. Energy consumption distribution with  $C = 20.66 \text{ kJ/}^{\circ}\text{C}$

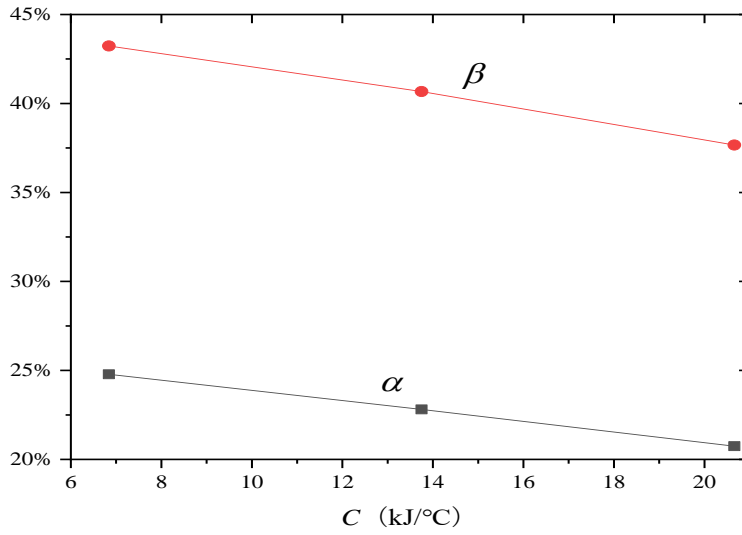


Fig. 11. Effects of  $C$  on  $\alpha$  and  $\beta$

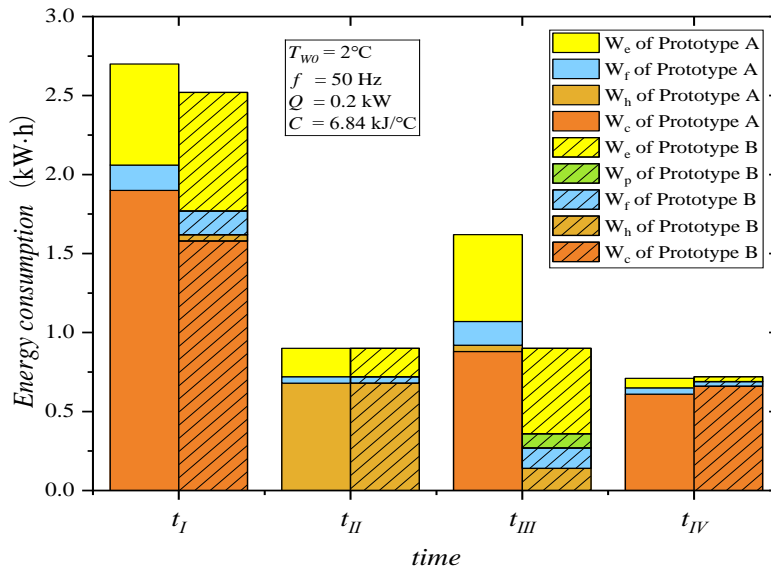


Fig. 12. Energy consumption distribution with  $Q = 0.2 \text{ kW}$

According to Fig. 12,  $W_c$  and  $W_t$  are 3.39 kWh and 5.93 kWh for Prototype A, and 2.24 kWh and 5.04 kWh for Prototype B. Here  $\alpha = 15.0\%$  and  $\beta = 33.9\%$  which indicate a lower energy-saving performance than that with  $Q = 1$  kW. Actually, due to very small  $Q (= 0.2$  kW) and the cold storage effect in the insulation material, the compressor does not have to run for the overall  $t_{III}$  for Prototype A. It is recorded in the test that only 25 min compressor operating time is needed in Stage III for Prototype A, much less than  $t_{III}$  for  $Q = 1$  kW (Seen in Fig. 5). Here, less compressor operating time of Prototype A leads to lower  $\alpha$  and  $\beta$  according to Eqs. (1) and (2). The observation in Fig. 12 tells us that the cold storage effect in the insulation material (or the size of the chamber) is related to the energy-saving effect of the cold storage-based design, which needs more research.

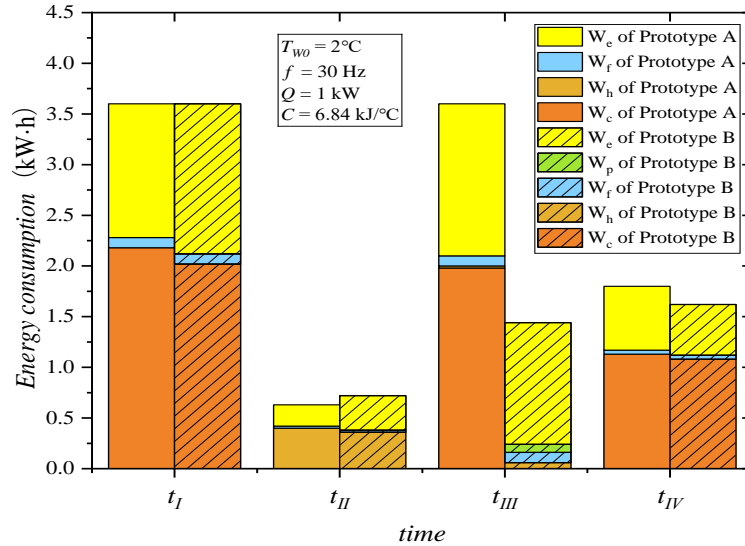


Fig. 13. Energy consumption distribution with  $f = 30$  Hz

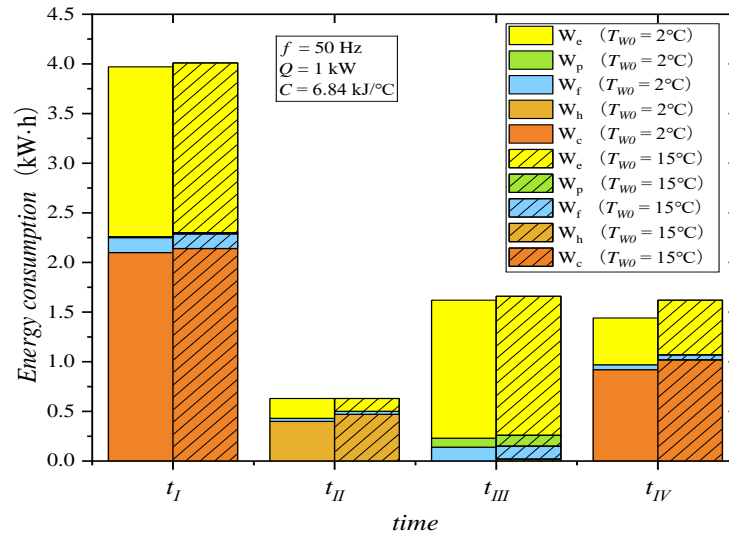


Fig. 14. Energy consumption distribution for Prototype B with  $T_{w0} = 15^\circ\text{C}$

In Section 3.1, the fan runs with frequency  $f = 50$  Hz. Through inverter control, the frequency  $f$  or the circulating air flow rate in the chamber can be adjusted. Figure 13 shows the energy consumption distribution for  $f = 30$  Hz. With the decrease of  $f$  from 50 Hz to 30 Hz,  $W_f$  reduces from 0.37 kWh to 0.26 kWh. Here, when  $f = 30$  Hz,  $W_c$  and  $W_t$  are 5.29 kWh and 9.63 kWh for Prototype A, and 3.10 kWh and 7.38 kWh for Prototype B. Both  $\alpha (= 23.4\%)$  and  $\beta (= 41.4\%)$  are slightly lower than that with  $f = 50$  Hz. We know that  $f$  affects not only  $W_f$  but also the heat transfer coefficients of CHE and EVA. The values of  $\alpha$  and  $\beta$  are the final results of these effects. It should be noted that the conclusion is only suitable for the present designs and cannot be extended to the conditions with very low fan frequency. In fact, when  $f$  is very low, the heat transfer areas of EVA and CHE may not

be sufficient, and the heat transfer between OBJ and the air will become worse too. The optimal air flow rate (corresponding to  $f$ ) is not the work of the present paper, but should be considered in real designs.

We have shown (in Fig. 7) that  $T_w$  may change in Stage III because for the present Prototype B we did not consider sufficient heat transfer enhancement in CST that may realize constant water temperature. The initial water temperature  $T_{w0}$  in Section 3.1 is 2°C. For Prototype B, by rising  $T_{w0}$  to 15°C, we performed similar test as in Section 3.1 under the nominal design conditions except different  $T_{w0}$ . The energy consumption distribution for  $T_{w0} = 15^\circ\text{C}$  for Prototype B is shown in Fig. 14. In this case,  $W_c$  and  $W_t$  rise to 3.16 kWh and 7.92 kWh, slightly higher than that for  $T_{w0} = 2^\circ\text{C}$ . This observation tells that variable  $T_{w0}$  does not affect the energy consumption significantly and constant  $T_w$  in CST design is not mandatory. Based on Fig. 14,  $\alpha$  and  $\beta$  are 22.2% and 40.6%, also slightly lower than that under nominal design condition (with  $T_{w0} = 2^\circ\text{C}$ ). It should be noted that higher  $T_{w0}$  means less heat transfer temperature difference in CHE, but we can still adjust the water flow rate to fulfill the design requirements for the present prototype (Prototype B).

### 3.3. Further Technical Discussion

In the above sections, we measured the energy-saving effect of the cold storage-based designs. Because ice and water are used as the cold storage substance and the coolant in CHE respectively, the stored cold energy cannot be utilized in Stage I or the part of Stage IV with  $T < T_w$ . Therefore, the present cold storage-based design (Prototype B) cannot reduce the size of the compressor or the refrigeration device. If low temperature substances ( $T < T_L$ ) to store cold energy are employed, the energy efficiency can be improved and the size of the compressor can be reduced simultaneously. Besides, we may further adopt two cold storage temperatures, for instance, one with coolant temperature  $T_{CS1}$  between  $T_H$  and  $T_L$  ( $T_L < T_{CS1} < T_H$ ), another with coolant temperature  $T_{CS2}$  ( $T_{CS2} < T_L$ ), schematically shown in Fig. 15. The coolant with  $T_{CS2}$  is used to burden a part of the cooling capacity demand in Stage IV, therefore the size of the compressor can be reduced. The above design with two cold storage temperatures also decreases the average temperature difference between the supply and the demand (or the entropy generation induced by heat transfer), besides it also increases the average coefficient of performance of the refrigeration device. More analysis is available in Ref. [5].

Additionally, even only one cold storage temperature with coolant temperature  $T_w > 0^\circ\text{C}$  provides the possibility in reducing the size of the compressor. For instance, the cold water from CST can be used to sub cool the refrigerant at the outlet of the condenser and increase the cooling capacity supply. If the cooling capacity demand is specified, we can therefore reduce the size of the compressor.

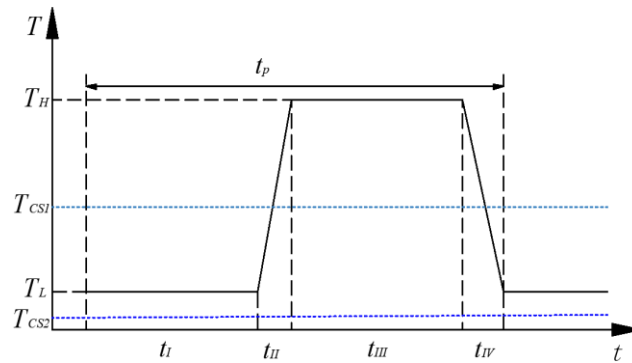


Fig. 15. The scheme of two cold storage temperatures

It is reminded that Fig. 15 shows the scheme of the two-scale design, i.e., the design with two coolant temperatures ( $T_{CS1}$  and  $T_{CS2}$ ) or cold storage temperature. In Fig. 1,  $T_L < T_{CS0} = 0^\circ\text{C}$  (the melting temperature of ice), where  $T_{CS0}$  represents the merely cold storage temperature (the one-scale design) in the experimental system in Section 2.

In Section 1, we mentioned that some studies showed that the incorporation of cold storage reduces the compressor operating time and therefore decreases the energy consumption. These studies mainly focused on normal air conditioning systems and refrigerators. The cooling load feature and the supply method of the cold storage energy in this paper are different from that in the literature, so it is difficult to compare them directly. In our previous theoretical analysis in Ref. [39], typical  $\alpha$  value is higher than 30%. But it is reminded that in Ref. [39],  $W_e$  is not considered, which is shown to be significant in this paper. Besides, the geometries of the prototypes used in this paper are not the same due to the consideration of manufacture and cost. Therefore, it is not proper to compare the experimental data (e.g.,  $\alpha$ ) with the simulation results in Ref. [39] quantitatively. Nevertheless, it is clear that the experimental results in this paper are in agreement with the theoretical design in Ref. [39] qualitatively.

### 3.4. Brief Economic Analysis

One important application of the systems in Fig. 2 is the reliability test of electronic and electrical devices, which usually needs long-time operation. As a case study, the lab-scale prototypes A and B in this paper consume 10.17 kWh/period and 7.66 kWh/period electricity respectively (cf. Section 3.1) under the specified nominal design conditions. In one year's, continuous operation (8760 h), compared with Prototype A, the energy-saving of Prototype B is around 8245 kWh.

On the other side, the investment of Prototype B is increased, including the cold storage tank, the coolant heat exchanger, the pump, more sensors, etc. In addition, the operation and maintenance are more complicated. For instance, when the temperature in the chamber is lower than 0°C (e.g., in Stage I), the water (i.e., the coolant) in the coolant heat exchanger should be discharged completely to avoid possible freezing damage. For the lab-scale Prototype B, the additional investment is limited [40]. For large-scale industrial applications, both the profit in energy-saving and the additional investment are significant. The trade-off depends on many factors, like users' demand, manufacturing level, electricity price, among others, which are beyond the scope of this paper.

## 4. Conclusions

In this work we developed two alternate temperature system prototypes with or without cold storage unit and presented the energy-saving effect of the cold storage-based design based on experimental results. The cold storage energy comes from a part of the refrigerant bypass loss. Under the specified nominal design conditions, the compressor consumes 5.32 kWh/period energy for the design without cold storage, while it consumes only 3.77 kWh/period energy for the design with cold storage due to less compressor operating time. Compared with the design without cold storage, the energy consumption reduction ratio ( $\alpha$ ) of the design with cold storage reaches approximately 24.7%. When the heat capacity of the load increases, e.g., from 6.84 kJ/°C to 20.66 kJ/°C, the energy-saving effect of the design with cold storage becomes weaker, e.g.,  $\alpha$  decreasing from 24.7% to 20.8% accordingly. For extremely low heat generation in the load, the energy-saving effect of the design with cold storage diminishes. The fan's operating frequency and the cold-water temperature, which are important for the design of the heat exchangers of the prototypes, affect the energy consumption reduction ratio slightly for the specified conditions.

It should be acknowledged that the present prototypes are preliminary, i.e., not fully optimized. There is great space for improvement, e.g., in reducing  $W_e$ . The important point is that the incorporation of one or more cold storage temperatures offer new design degrees of freedom which increases the possibility of evolving design toward better performance or less entropy generation (e.g., due to the heat transfer between the coolant and the air). If the size reduction of the compressor is not considered, e.g., Prototype B in this work, cold storage also implies higher investment and more complicated control, so trade-off is always necessary in real product development. If the size of compressor is reduced as analyzed in Section 3.3, the investment may not increase. More product development and test are worthy.

## Nomenclature

C	heat capacity [JK <sup>-1</sup> ]
f	fan's operating frequency [Hz]
$\dot{m}_w$	water flow rate [Lmin <sup>-1</sup> , m <sup>3</sup> h <sup>-1</sup> ]
Q	heat transfer rate [W, kW]
T	temperature [°C, K]
t	time [s]
T <sub>0</sub>	ambient temperature [°C, K]
u	relative uncertainty
W	energy consumption or work [J, kJ, MJ]

### Greek symbols

$\alpha$	energy consumption reduction ratio
$\beta$	compressor work reduction ratio
$\delta$	absolute uncertainty

### Subscripts

0	initial
I, II, III, IV	Stages I, II, III, IV
A, B	Prototype A, B
c	compressor
CS0, CS1, CS2	cold storage temperature 0,1, 2
e	other energy consumption
f	fan
H	high
h	heater
L	low
p	pump
t	total
w	water

### Abbreviations

CHAM	the chamber
CHE	the coolant heat exchanger
COM	the compressor
CON	the condenser
CST	the cold storage tank
EV	the expansion valve
EVA	the evaporator
FAN	the fan
HT	the heater
IHE	the ice-generating heat exchanger
OBJ	the object
V, V1, V2, V3	valves in Fig. 2

## References

- [1] Garimella SV, Fleischer AS, Murthy JY, Keshavarzi A, Prasher R, Patel C, Bhavnani SH, Venkatasubramanian R, Mahajan R, Joshi Y, Sammakia B, Myers BA, Chorosinski L, Baelmans M, Sathyamurthy P, Raad PE. Thermal Challenges in Next-Generation Electronic Systems. *IEEE Transactions on Components and Packaging Technologies*, 2008;31(4):801-15. <https://doi.org/10.1109/TCAPT.2008.2001197>
- [2] Steinberg DS. *Preventing Thermal Cycling and Vibration Failures in Electronic Equipment*. Wiley, 2001, ISBN 978-0-471-35729-2.
- [3] Yang S, Bryant A, Mawby P, Xiang D, Ran L, Tavner P. An Industry-Based Survey of Reliability in Power Electronic Converters. *IEEE Transactions on Industry Applications*, 2011;47(3):1441-51. <https://doi.org/10.1109/TIA.2011.2124436>
- [4] Chen X, Zhang C, Wang Y, Tan Y. *Accelerated Life Testing Technology and Applications*. National Defence Industry Press, Beijing, China, 2013.

- [5] Zhang H, Zhou R, Lorente S, Ginestet S. Thermodynamic design of cold storage-based alternate temperature systems. Applied Thermal Engineering, 2018;144:736-46. <https://doi.org/10.1016/j.applthermaleng.2018.08.099>
- [6] Selimli S, Recebli S, Görken M. Evaluation the effects of used refrigerants R134a and R600a in cooling systems on the system performance. Journal of Engineering and Natural Sciences, 2014; Sigma 32: 290-295.
- [7] Patiluna DNG, Donasco EAA, Hernandez NM, Mamalias JBA, Viña RR. Energy and exergy analysis of a two-stage cascade vapor compression refrigeration system with modified system configuration. International Journal of Refrigeration, 2025;169:33-54. <https://doi.org/10.1016/j.ijrefrig.2024.10.013>
- [8] Widell KN, Eikevik T. Reducing power consumption in multi-compressor refrigeration systems. International Journal of Refrigeration, 2010;33(1):88-94. <https://doi.org/10.1016/j.ijrefrig.2009.08.006>
- [9] Qureshi TQ, Tassou SA. Variable-speed capacity control in refrigeration systems. Applied Thermal Engineering, 1996;16(2):103-13. [https://doi.org/10.1016/1359-4311\(95\)00051-E](https://doi.org/10.1016/1359-4311(95)00051-E)
- [10] Li W. Simplified steady-state modeling for variable speed compressor. Applied Thermal Engineering, 2013;50(1):318-26. <https://doi.org/10.1016/j.applthermaleng.2012.08.041>
- [11] Li G, Hwang Y, Radermacher R. Review of cold storage materials for air conditioning application. International Journal of Refrigeration, 2012;35(8):2053-77. <https://doi.org/10.1016/j.ijrefrig.2012.06.003>
- [12] Zhai XQ, Wang XL, Wang T, Wang RZ. A review on phase change cold storage in air-conditioning system: Materials and applications. Renewable and Sustainable Energy Reviews, 2013;22:108-20. <https://doi.org/10.1016/j.rser.2013.02.013>
- [13] Kalnæs SE, Jelle BP. Phase change materials and products for building applications: A state-of-the-art review and future research opportunities. Energy and Buildings, 2015;94:150-76. <https://doi.org/10.1016/j.enbuild.2015.02.023>
- [14] Souayfane F, Fardoun F, Biwole P-H. Phase change materials (PCM) for cooling applications in buildings: A review. Energy and Buildings, 2016;129:396-431. <https://doi.org/10.1016/j.enbuild.2016.04.006>
- [15] Rahgozar S, Dehghan M, Pourrajabian A, Haghgou H. Economic feasibility of ice storage systems for office building applications: A climate sensitivity analysis. Journal of Energy Storage, 2022; 45:103712. <https://doi.org/10.1016/j.est.2021.103712>
- [16] Conti P, Franco A, Bartoli C, Testi D. A design methodology for thermal storages in heat pump systems to reduce partial-load losses. Applied Thermal Engineering, 2022;215:118971. <https://doi.org/10.1016/j.applthermaleng.2022.118971>
- [17] Zhu Y, Zhang Q, Zeng L, Wang J, Zou S. An advanced control strategy of hybrid cooling system with cold water storage system in data center. Energy, 2024;291:130304. <https://doi.org/10.1016/j.energy.2024.130304>
- [18] Zhao J, Liu D, Yuan X, Wang P. Model predictive control for the ice-storage air-conditioning system coupled with multi-objective optimization. Applied Thermal Engineering, 2024;243:122595. <https://doi.org/10.1016/j.applthermaleng.2024.122595>
- [19] Lin X, Shan K, Wang S. Model predictive control of large chiller plants for enhanced energy efficiency utilizing inherent cold storage of cooling systems. Journal of Energy Storage, 2025;113:115697. <https://doi.org/10.1016/j.est.2025.115697>
- [20] Azzouz K, Leducq D, Gobin D. Performance enhancement of a household refrigerator by addition of latent heat storage. International Journal of Refrigeration, 2008;31:892-901. <https://doi.org/10.1016/j.ijrefrig.2007.09.007>
- [21] Azzouz K, Leducq D, Gobin D. Enhancing the performance of household refrigerators with latent heat storage: An experimental investigation. International Journal of Refrigeration, 2009;32(7):1634-44. <https://doi.org/10.1016/j.ijrefrig.2009.03.012>
- [22] Marques AC, Davies GF, Evans JA, Maidment GG, Wood ID. Theoretical modelling and experimental investigation of a thermal energy storage refrigerator. Energy, 2013;55:457-65. <https://doi.org/10.1016/j.energy.2013.03.091>
- [23] Khan MIH, Afroz HMM. Effect of phase change material on performance of a household refrigerator. Asian Journal of Applied Sciences, 2013;6(2):56-67. <https://doi.org/10.3923/ajaps.2013.56.67>
- [24] Marques AC, Davies GF, Maidment GG, Evans JA, Wood ID. Novel design and performance enhancement of domestic refrigerators with thermal storage. Applied Thermal Engineering, 2014;63:511-519. <https://doi.org/10.1016/j.applthermaleng.2013.11.043>
- [25] Liu Z, Zhao D, Wang Q, Chi Y, Zhang L. Performance study on air-cooled household refrigerator with cold storage phase change materials. International Journal of Refrigeration, 2017;79:130-42. <https://doi.org/10.1016/j.ijrefrig.2017.04.009>
- [26] Ezan MA, Ozcan Doganay E, Yavuz FE, Tavman IH. A numerical study on the usage of phase change material (PCM) to prolong compressor off period in a beverage cooler. Energy Conversion and Management, 2017;142:95-106. <https://doi.org/10.1016/j.enconman.2017.03.032>

- [27] Cheng W, Ding M, Yuan X, Han B. Analysis of energy saving performance for household refrigerator with thermal storage of condenser and evaporator. *Energy Conversion and Management*, 2017;132:180-8. <https://doi.org/10.1016/j.enconman.2016.11.029>
- [28] Joybari M, Haghighat F, Moffat J, Sra P. Heat and cold storage using phase change materials in domestic refrigeration systems: The state-of-the-art review. *Energy and Buildings*, 2015;106:111-24. <https://doi.org/10.1016/j.enbuild.2015.06.016>
- [29] Liao Z, Zhuang C, Huang G, Pu H, Zhang H, Li S, Zhang X, Cheng L, Gan F. Optimization research on phase change cold storage module for refrigerated containers. *Journal of Energy Storage*, 2024;82:110506. <https://doi.org/10.1016/j.est.2024.110506>
- [30] Gao L, Xu S, Yu G, Ma G, Chang Y, Li S. Application study of direct current refrigerator combining phase-change cold storage and mini-electrical storage. *Energy*, 2025;320:135308. <https://doi.org/10.1016/j.energy.2025.135308>
- [31] Zhang L, Xia X, Lv Y, Wang F, Cheng C, Shen S, Yang L, Dong H, Zhao J, Song Y. Fundamental studies and emerging applications of phase change materials for cold storage in China. *Journal of Energy Storage*, 2023;72:108279. <https://doi.org/10.1016/j.est.2023.108279>
- [32] Ouaouja Z, Ousegui A, Toublanc C, Rouaud O, Havet M. Phase Change Materials for Cold Thermal Energy Storage applications: A critical review of conventional materials and the potential of bio-based alternatives. *Journal of Energy Storage*, 2025;110:115339. <https://doi.org/10.1016/j.est.2025.115339>
- [33] Bejan A. Constructal-theory network of conducting paths for cooling a heat generating volume. *International Journal of Heat and Mass Transfer*, 1997;40(4):799-816. [https://doi.org/10.1016/0017-9310\(96\)00175-5](https://doi.org/10.1016/0017-9310(96)00175-5)
- [34] Bejan A, Lorente S. *Design with Constructal Theory*. Wiley, 2008, ISBN 978-0-471-99816-7. <https://doi.org/10.1002/9780470432709>
- [35] Radcenco V, Vargas JVC, Bejan A, Lim JS. Two design aspects of defrosting refrigerators. *International Journal of Refrigeration*, 1995;18(2):76-86. [https://doi.org/10.1016/0140-7007\(94\)00003-G](https://doi.org/10.1016/0140-7007(94)00003-G)
- [36] Zamfirescu C, Bejan A. Tree-shaped structures for cold storage. *International Journal of Refrigeration*, 2005;28(2):231-41. <https://doi.org/10.1016/j.ijrefrig.2004.08.010>
- [37] Bi Y, Guo T, Zhang L, Chen L, Sun F. Entropy generation minimization for charging and discharging processes in a gas-hydrate cool storage system. *Applied Energy*, 2010;87(4):1149-57. <https://doi.org/10.1016/j.apenergy.2009.07.020>
- [38] Tavakoli A, Farzaneh-Gord M, Ebrahimi-Moghadam A. Using internal sinusoidal fins and phase change material for performance enhancement of thermal energy storage systems: Heat transfer and entropy generation analyses. *Renewable Energy*, 2023;205:222-37. <https://doi.org/10.1016/j.renene.2023.01.074>
- [39] Zhou R, Tu P, Zhang H. Performance improvement of alternate temperature systems with ice storage-based internal water loop. *Energy and Buildings*, 2019;204:109521. <https://doi.org/10.1016/j.enbuild.2019.109521>
- [40] Zhu L. Study on performance optimization of high and low temperature test chambers (Thesis, in Chinese). Nanjing University of Science and Technology, China, 2021.
- [41] Moffat RJ. Describing the uncertainties in experimental results. *Experimental Thermal and Fluid Science*. 1988;1(1):3-17. [https://doi.org/10.1016/0894-1777\(88\)90043-X](https://doi.org/10.1016/0894-1777(88)90043-X)